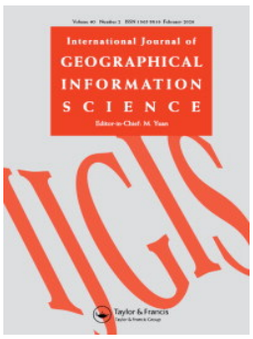

International Journal of Geographical Information Science

ISSN: 1365-8816 (Print) 1362-3087 (Online) Journal homepage: www.tandfonline.com/journals/tgis20

Measuring univariate effects in the interaction of geographical patterns

Peng Luo, Yang Li, Yongze Song, Ziqi Li & Liqiu Meng

To cite this article: Peng Luo, Yang Li, Yongze Song, Ziqi Li & Liqiu Meng (2026) Measuring univariate effects in the interaction of geographical patterns, International Journal of Geographical Information Science, 40:2, 382-413, DOI: 10.1080/13658816.2025.2526042

To link to this article: https://doi.org/10.1080/13658816.2025.2526042

Published online: 07 Jul 2025.

INTERNATIONAL JOURNAL OF GEOGRAPHICAL INFORMATION SCIENCE
2026, VOL. 40, NO. 2, 382–413
https://doi.org/10.1080/13658816.2025.2526042

Taylor & Francis
Taylor & Francis Group

RESEARCH ARTICLE

OPEN ACCESS Check for updates

Measuring univariate effects in the interaction of geographical patterns

Peng Luo[a], Yang Li[b], Yongze Song[c], Ziqi Li[d] and Liqiu Meng[e]

[a]Senseable City Lab, Massachusetts Institute of Technology, Cambridge, MA, USA; [b]Hangzhou International Innovation Institute, Beihang University, Hangzhou, China; [c]School of Design and the Built Environment, Curtin University, Perth, Australia; [d]Department of Geography, Florida State University, Tallahassee, FL, USA; [e]Chair of Cartography and Visual Analytics, Technical University of Munich, Munich, Germany

ABSTRACT

Understanding the relationships between geographical variables is a fundamental task in spatial analysis. However, existing spatial methods often underperform in scenarios involving nonlinear relationships and complex interactions among geographical variables. Identifying the relationships between individual variables (i.e. univariate effect) within multiple interacting variables remains challenging and long-lasting. In this study, we propose a novel model—Geographical Pattern Interaction (GPI)—based on the premise that the spatial pattern of a response variable emerges from the interaction of spatial patterns in explanatory variables. GPI leverages decision trees and Shapley value explanations to quantify both global and local univariate effects by measuring the alignment between the spatial distribution of the target variable and those of the predictors. Through simulation experiments, we demonstrate GPI's superior performance compared to traditional regression-based spatial explanation methods. Notably, the GPI framework is stable across varying spatial scales and sample sizes, making it particularly suitable for spatial explanation tasks under small data and multi-scale conditions. A case study on homelessness risk in Australia demonstrates GPI's ability to reveal nonlinear spatial associations and interaction effects. By capturing overlooked pattern similarities and interactions, GPI offers an interpretable and transferable tool for analyzing complex spatial relationships.

ARTICLE HISTORY
Received 25 December 2023
Accepted 23 June 2025

KEYWORDS
Spatial association; spatial heterogeneity; nonlinear interaction; geographical pattern interaction

1. Introduction

One of the primary tasks in geographical analysis is to determine the relationships between geographical variables (Anselin 1988; Brunsdon *et al.* 1996). Analyzing these relationships can help understand underlying data generating processes, predict future scenarios, and inform decision making. Quantitative relationships can be measured through statistical models applied to geographical data (Fotheringham *et al.* 2000;

CONTACT Yang Li isliyang@buaa.edu.cn; Yongze Song yongze.song@curtin.edu.au

LeSage and Fischer 2008). Traditional statistical models are often used to identify non-spatial relationships. Parameter estimation by using geographical samples collected from different locations, and assuming a constant relationship among geographical variables across space, however, may, result in biased results and violated assumptions. Spatial statistical approaches have been developed to explicitly address possible spatial effects present in the data (Song 2023). Spatial effects are normally classified into spatial dependence (Anselin 1988) and spatial heterogeneity (Fotheringham *et al.* 2003; Goodchild 2004). Spatial dependence refers to the correlation that exists between neighboring locations in geographic space, which reflects the tendency of geographical phenomena to cluster or disperse in space, and can often be captured through spatial regression models (Anselin 1995; Luo *et al.* 2023; Lou *et al.* 2024). Spatial heterogeneity, on the other hand, indicates that the process generating the data may vary across different locations (Getis and Ord 1992; De Marsily *et al.* 2005; Fotheringham *et al.* 2003). This heterogeneity may manifest that geographical phenomena exhibit different characteristics or patterns at different locations (Luo and Song 2021). Spatial heterogeneity can be modeled in either a discrete or continuous manner (Zhang *et al.* 2024). Multi-level models and spatial regimes are often used to address discrete heterogeneity (Wang and Xu 2017; Fotheringham and Li 2023; Anselin and Amaral 2024), while continuous heterogeneity can be modeled using spatially varying coefficients models, such as Geographically Weighted Regression (GWR) (Fotheringham *et al.* 2003) and Spatial Eigenvector Filtering (Griffith 2003).

Previous spatial models are predominantly constructed based on the two spatial effects mentioned above to reveal spatial association, but there remain some unresolved issues. First, they often ignore the complex interactions among explanatory variables (Song *et al.* 2020; Zhang *et al.* 2023), and require that the residuals from different observations are independent (Anselin 1989). The spatial distribution of geographical variables can be influenced by the interaction of multiple explanatory variables. For example, the function between the response variable and an individual explanatory variable X_a, as represented by $f(X_a)$ may include interactions with other variables (e.g. X_b): $f(X_a \cap X_b)$. It is crucial to comprehend how individual variables relate to one another (the univariate effect) when there are several interacting variables at play. Ignoring the interaction among variables could cause the univariate effect to be over- or underestimated. Second, current spatial models heavily rely on linearity assumptions (Comber *et al.* 2021; Li 2022). The relationships between geographical variables often exhibit significant non-linearity. For instance, a moderate increase in temperature can enhance the growth of certain plants, but excessively high temperatures may inhibit their growth (Zhu *et al.* 2021). Third, current models often impose strict statistical assumptions on data distribution (e.g. Normal, Poisson), which are usually violated in real geospatial dataset (Arbia 2006). Geographical data is often influenced by spatial dependency resulting in non-i.i.d. (independent and identically distributed) samples. In summary, current spatial models for detecting relationships commonly overlook variable interaction effects and impose inflexible statistical assumptions on functional forms (e.g. linearity) and data distributions.

The limitations mentioned above arise from the modeling approach to spatial effects. Most models for detecting spatial relationships assume that spatial effects,

such as spatial heterogeneity, are continuously present across space. They rely on the values of geographical variables at each sample point to model the relationships between them. However, in reality, spatial heterogeneity can be modeled not only continuously across geographical space but also discretely (Anselin and Amaral 2024). Concepts such as spatial regimes and stratified spatial heterogeneity (SSH) have been introduced to describe this discrete heterogeneity (Anselin 2010; Hu *et al.* 2025). Within the theoretical framework for discretely modeling spatial heterogeneity, regions with heterogeneity are subdivided into multiple homogeneous subregions (Guo *et al.* 2023). In each subregion, model parameters remain consistent, indicating a presumed stationary spatial relationship.

This study models discrete spatial heterogeneity to identify spatial correlations, with the expectation of not imposing overly strong statistical assumptions on spatial data. We introduce a new way of thinking about spatial relationships in line with people's intuitive understanding of the geospatial world: the more similar the spatial distribution patterns of two geographical variables, the stronger their relationship may be. The extent to which an explanatory variable X's spatial distribution influences the spatial distribution of the response variable Y can reflect their correlation. Our aim is to incorporate this assumption into spatial correlation analysis by evaluating the spatial pattern similarity among geographical variables to analyze their mutual relationships and interaction strength.

In addition to proposing relatively loose statistical assumptions, we attempt to be able to reveal interactions among multiple explanatory variables. The geographically optimal zones-based heterogeneity model (GOZH) was developed to address this issue (Luo *et al.* 2022). It is one of the most advanced SSH models and has been proven effective in identifying spatial associations by detecting the spatial patterns of geographical variables. Its purpose is to achieve geographically optimal zones for every combination of variables and to determine the geographically optimal partition given all explanatory variables (Luo *et al.* 2025). GOZH does not rely on statistical assumptions about data distribution, such as assuming a normal distribution. Furthermore, GOZH has the capability to detect non-linear relationships between variables (Yang *et al.* 2024).

However, GOZH cannot reveal global univariate effects under conditions of pattern interaction. It can provide an overall assessment of the combined impact of multiple explanatory variables on the response variable, but it cannot calculate the individual contribution of a specific variable within this interaction. Secondly, it cannot explore the local univariate effects under conditions of pattern interaction. One of the key distinctions between models based on discrete heterogeneity (e.g. GOZH model) and models based on continuous heterogeneity (e.g. GWR model) is that the former cannot estimate local spatial non-stationary parameters. Due to this limitation, GOZH cannot explore the spatially varying relationships.

Based on the above discussion, there is a critical need to develop a new approach for measuring univariate effects in the interaction of geographical patterns. This approach should simultaneously achieve two main objectives: (i) to identify the overall correlation between explanatory variables and response variables (global effect), and (ii) to reveal the spatially varying relationship (local effect).

Consequently, this study develops a geographical pattern interaction (GPI) model to identify the univariate effects under the condition of pattern interaction. GPI model works in three steps. The first step is to generate the clustering pattern of the response variable given the spatial pattern of multiple explanatory variables. Within each cluster unit, the values of the response variable are similar. Different clustering methods can be used to identify clustering patterns based on the values of explanatory variables, such as K-means, SVM-based methods, or decision tree-based methods, where GOZH model is applied. The second is to calculate the global univariate effects in GPI. For each geographic discretization under each combination of variables, we calculate the variance of each partition and the overall relationship between the explanatory and response variables. This analysis includes the interaction between a single explanatory variable and multiple explanatory variables, using the concept of spatially stratified heterogeneity. We then introduce Shapley value, an interpretable algorithm based on game theory, to quantify the contribution of a single variable in the interaction of multiple explanatory variables (Štrumbelj and Kononenko 2014; Lundberg *et al.* 2020; Li 2022; Li *et al.* 2023; Li *et al.* 2023). This process follows the locally explained stratified heterogeneity (LESH) model, which relies on decision tree-based explanations to refine GOZH methods for better interpretability (Li *et al.* 2023). The third is to calculate local univariate effects in GPI, including local effects of GPI, local univariate effects, and their characteristics of nonlinearity, local dominant variables, and bi-variate effects. We computed the means of the response variables for each geographical partition of the region under different combinations of variables, and then used Shapley value based method to explore the contribution of different variables to the classification of the region as a geographically optimal partition. This contribution represents the relationship between the explanatory variables and the response variables in this region.

The remainder of this paper is organized as follows: Section 2 introduces the concept and framework of the GPI model; Section 3 designs three sets of experiments on the simulated dataset; Section 4 presents a case study of applying the GPI to analyze the risk of homelessness in Australia; Section 5 demonstrates the results of the case study. We discuss the methodological contributions of the GPI in Section 6 and conclude the study in Section 7.

2. Geographical pattern interaction (GPI)

2.1. The definition of GPI model

The GPI model identifies relationships between geographical variables by analyzing similarities in their spatial distributions, integrating both global and local spatial relationships for the pattern interaction analysis.

To understand the relationship between explanatory variables and the response variable, we first partition the spatial domain of the response variable using a combination of all explanatory variables, resulting in pattern M. Subsequently, we segment the response variable based on different subsets of explanatory variables or individual variables (assuming there are n such combinations), yielding patterns $M'_1, M'_2, \ldots, M'_n$. We then assess the contribution of different variable combinations to the response

variable. We argue that the closer a spatial pattern M' (generated by a given set of explanatory variables) is to M, the more important that set of explanatory variables is for determining the response variable Y. Finally, we introduce the concept of game theory (specifically, the Shapley value in practical implementation) to decompose the contribution of variable combinations into the contributions of individual variables. This decomposition includes both the overall spatial impact of an individual variable and its contribution at each specific location.

A key step in the GPI computational framework is how to measure the similarity between two patterns (M' and M). In GPI, the total between-group variance across different grouping methods is used to quantify the overall similarity between the two patterns, which aligns with the SSH methodology. In addition, the differences in mean values of subregions across different combinations are used to represent their local similarity.

2.2. The hypothesis underlying GPI model

The essence of GPI model is based on the hypothesis that the interaction between geographical patterns can indicate spatial association. The distribution of the response variable is determined by a series of interactions among multiple explanatory variables. For a specific explanatory variable X, its impact on the spatial pattern of the response variable Y represents the spatial association between X and Y. Spatial pattern can be characterized in various ways. Normally, the distribution of a geographical variable exhibits a spatial pattern: it values can be grouped into several relatively homogeneous subregions, where values are similar within each subregion and dissimilar between different subregions (Anselin and Amaral 2024). The proper description of the spatial pattern of each geographic variable can facilitate the exploration of their spatial association. We find that the stronger the spatial pattern interaction driven by explanatory variables, i.e. higher similarity within subregions and greater dissimilarity between subregions in the spatial pattern of the response variable, the stronger the spatial association between these explanatory variables and the response variable.

For instance, we are interested in understanding the association between elevation (explanatory variable) and temperature (response variable). We divide the area based on elevation into high-elevation and low-elevation regions. When we observe that high-elevation regions generally have lower temperatures, and low-elevation regions generally have higher temperatures, it is reasonable to infer that temperature is strongly influenced by (or associated with) elevation.

More often, a geographical phenomenon of interest is associated with multiple explanatory variables and their spatial associations can be determined in a similar manner as shown in Figure 1. Suppose the response variable Y is determined by two explanatory variables, X_a and X_b. The value of the response variable, Y, is indicated by the color value, while explanatory variables X_a and X_b are distinguished by different color hues to represent different distributions or categories of values. For example, three regions of X_a—red, blue, and green—may represent three different states or levels of the variable. We can determine the geographic interaction patterns of Y based on X_a, X_b, and the interaction between X_a and X_b. The distribution of X_a allows for the

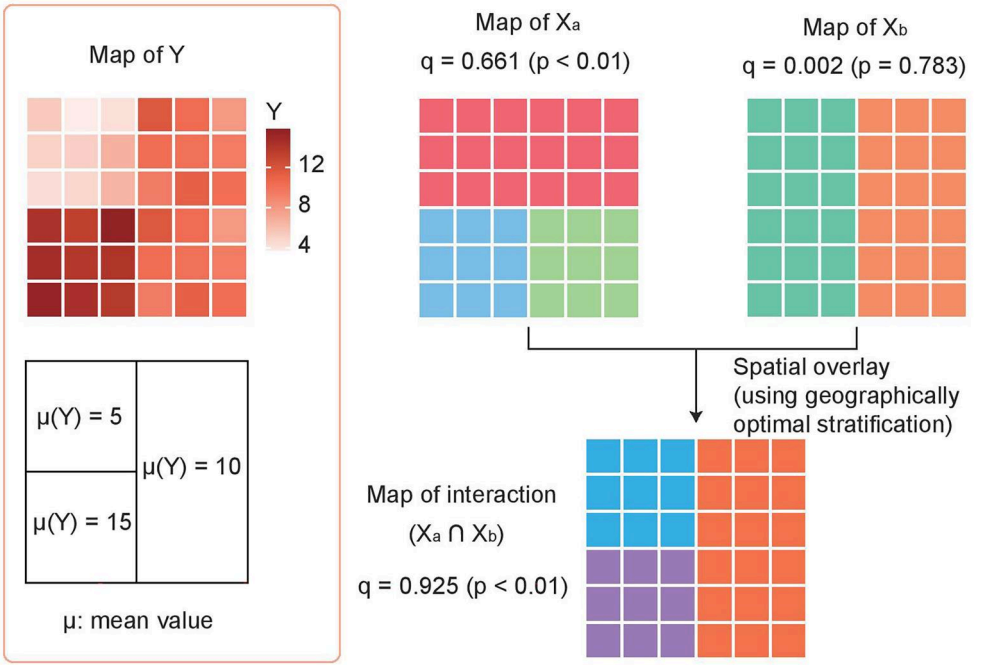

Figure 1. An example of identifying the spatial association according to the pattern interaction. The black lines represent the division of the response variable space based on explanatory variables.

spatial division of Y into three regions, with mean values of 7.5, 15, and 10, respectively. We utilize the index q to assess the spatial stratification heterogeneity of this case, which measures the extent to which the spatial distribution of X can explain (i.e. distinguish) the distribution of Y. The q value for X_a is 0.661 with a p-value of less than 0.01, indicating a significant spatial association between X_a and Y. On the other hand, based on X_b's distribution, Y is divided into two subregions with a mean value of 10, indicating that X_b alone is ineffective in distinctly discretization Y. The q-value for X_b is 0.002 with a p-value of 0.783, suggesting no significant spatial association with Y. However, when X_a and X_b interact, the geographic pattern of Y is divided into three subregions with mean values of 5, 15, and 10, achieving a perfect separation. The q-value is 0.925 with a p-value of less than 0.01, implying a very strong spatial association between Y and the combination of X_a and X_b. This demonstrates that the collaborative interaction of X_a and X_b can explain 92.5% of the spatial variability in Y. It also indicates that some explanatory variables, like X_b, cannot independently affect the response variable. However, when they interact with other variables, their explanatory power is significantly enhanced. This phenomenon is common in the field of geography but has not been well addressed with previous models. SSH-based models, such as geographical detector (Wang *et al.* 2010) and optimal parameters-based geographical detector (OPGD) (Song *et al.* 2020) account for the interaction effect between multiple variables but cannot reveal spatially varying interactions.

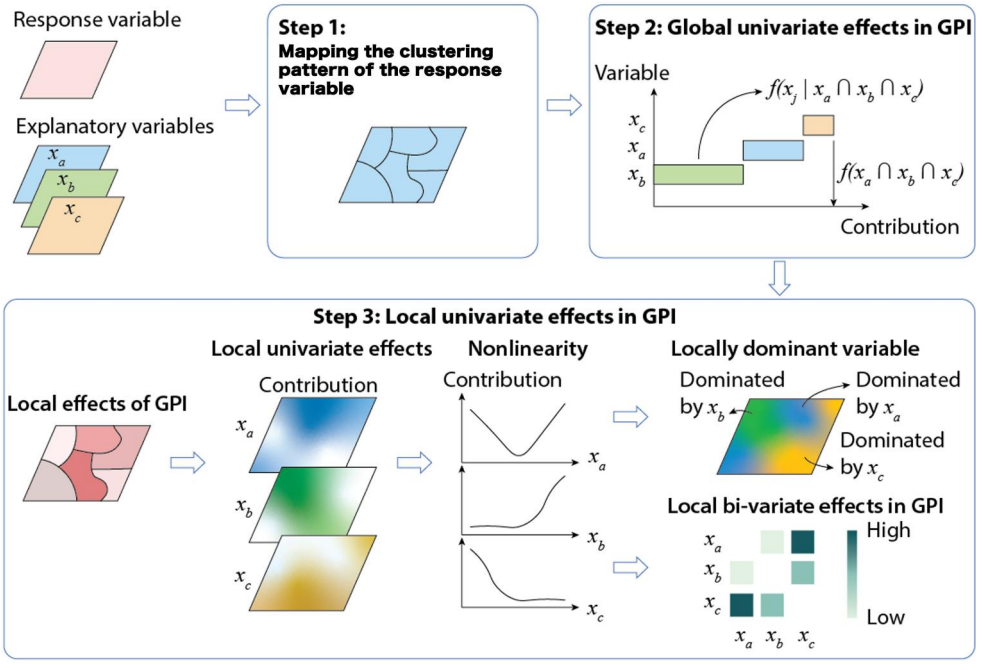

Figure 2. Flowchart of geographical pattern interaction (GPI) model.

2.3. The workflow of GPI model

Figure 2 shows the framework of the GPI model designed to explore the interaction of distribution patterns among geographical variables, including both global and local spatial relationships among various variables, and to assess the impact of each individual variable within this interaction. In the framework, a response variable and three explanatory variables are annotated as Y and X_a, X_b, and X_c.

In the first step, the model generates the clustering pattern of the response variable. The spatial distribution of Y is divided into several homogeneous subzones given the interaction of the explanatory variables. The model is able to minimize the sum of the within-zone variance of the response variable across all subzones. In the second step, the model calculates the global univariate effects in the GPI. It reveals the overall impact of each explanatory variable on the response variable. It also detects the contribution of each explanatory variable in the GPI.

In the third step, the model detects the local univariate effects in GPI. Firstly, the spatial distribution of local effects of GPI is mapped. Secondly, at each spatial position, the model discerns the spatial correlation between each individual variable X and the response variable Y. In this manner, the spatial distribution of these correlations can be visualized. Thirdly, the model explores the nonlinearity of the contribution of each explanatory variable. Fourthly, the locally dominant variable is detected which represent the explanatory variable with the strongest association with the response variable. Finally, at each specific location, the model delves into the interactive effects of different variables.

2.3.1. Generation of clustering pattern

The first step of GPI is to map the clustering pattern of the response variable, which is defined as homogeneous regions derived from its spatial distribution. Ideally, the homogeneity within each region should ideally approach optimality (Luo *et al.* 2021). The model should minimize the total variance among these regions, as is measured by the PD value:

$$PD(X) = \min(SSW_{X,D}) = \min\left\{\sum_{z=1}^{h}\sum_{j=1}^{N_z}(y_{z,j} - \overline{c}_z)^2\right\} \tag{1}$$

where X is one or multiple explanatory variables, D is the stratified variable for describing geographical strata, and $SSW_{X,D}$ is the sum of squares within geographical strata that are recorded as D and determined by explanatory variable X. $y_{z,j}$ and $\overline{c}_z$ are the jth observation and mean values of response variables in stratum z, respectively.

In GPI, the selection of the spatial discretization method depends on the specific research questions and the characteristics of the data. For more details on the spatial discretization process, please refer to the GOZH model (Luo *et al.* 2022). In this study, we employ CART for spatial discretization, as decision tree-based models provide strong interpretability.

$$\min_{k,s}\left\{\sum_{x_i \in Z_1(k,s)}(y_i - \overline{d}_1)^2 + \sum_{x_i \in Z_2(k,s)}(y_i - \overline{d}_2)^2\right\} \tag{2}$$

where k represents the index of the explanatory variable being analyzed, s represents the optimal cutoff point for the explanatory variable X_k, $\overline{d}_1$ and $\overline{d}_2$ are the average values of response variable in subzone Z_1 and Z_2, respectively.

2.3.2. Global univariate effects

Global geographical association (for whole study area **u**) between explanatory variable X_j and Y is descripted as:

$$G = f(X_j(\mathbf{u})|X_1 \cap X_2 \cap \ldots \cap X_n) = \varphi_{X_j}(PD) \tag{3}$$

where $\mathbf{u} = [u]$, indicates the whole study area containing all location u, $f(x)$ is the impact of geo-interaction, φ is the function to calculate the contribution of a single explanatory variable. In this study, we specifically apply the idea of SHAP (SHapley Additive exPlanations) to quantify the univariate contribution to the response variable. SHAP is a method to fairly distribute the 'payout' among players in game theory (Shapley *et al.* 1953; Lundberg *et al.* 2017). This method assigns each feature an importance value, showing how much it influences the output. It works by comparing predictions with and without each feature, averaging these differences across all possible combinations. It can be calculated as:

$$\varphi_{X_j}(PD) = \left|\sum_{S \subseteq C\ \{X_j\}} \frac{|S|!(|C| - |S| - 1)!}{|C|!}\left(PD(S \cup \{X_j\}) - PD(S)\right)\right| \tag{4}$$

where, C is a set of all variables, S is a subset of C. $|S|$ and $|C|$ represent the number of variables in the set.

Specifically, we iterate through all possible variable combinations ($2^{|C|-1}$ combinations in total) to compute the PD value based on formula (1) and (2). Then, the univariate effects are calculated as in formula (4). The $\varphi_{X_j}(PD)$ is the weighted average of the gain in PD values attributable to variable X_j under all combinations. In the end, Shapley value of the PD of each variable is calculated to quantify the effect of this variable under GPI.

2.3.3. Local univariate effects

Local univariate effects contain five components: (i) overall local effects (average value of each subzone); (ii) local univariate effects under the condition of GPI; (iii) nonlinearity of local univariate effects; (iv) identifying predominant local variables; and (v) local interaction effects under the condition of GPI.

The first component is the overall local effects. The local effect is the average of the Y values over the stratum z. To all specific locations over the stratum z, the local effect of a combination of explanatory variable $C(x_1, x_2 \ldots x_j | 1 \leq j \leq n)$ are the same and are calculated as:

$$I_u(C) = \frac{\mathrm{Sum}_z(Y)}{n_z} \tag{5}$$

where z is a stratum of the study area, u is the location of a sample within stratum z, and n represents the number of samples within stratum z.

The second component is employing Shapley values to calculate local univariate effects under the condition of GPI, which is descripted as:

$$L = f(X_j(u)|X_1 \cap X_2 \cap \ldots \cap X_n) = \varphi(I_u) \tag{6}$$

where $f(x)$ is the impact of geo-interaction, φ is the function to calculate the contribution of a single explanatory variable. We also apply the Shapley values to quantify the local univariate effects. The difference between the calculation of the global univariate effect is that, in this case, the input is an indicator used to describe the local spatial pattern in location u (as specified in formula (5)). Therefore, the univariate effects for each location are calculated as follows:

$$\varphi_{x_j}(I_u) = \sum\nolimits_{S \subseteq C \ \{x_j\}} \frac{|S|!(|C| - |S| - 1)!}{|C|!} \left(I_u\left(S \cup \{x_j\}\right) - I_u(S) \right) \tag{7}$$

where u is a location.

Thirdly, we explore the non-linear relationships between variables. We group the explanatory variables using quantiles and then examined the corresponding local Shapley values. This allows us to obtain non-linear impact curves of the explanatory variables on the dependent variable. Fourthly, we calculate the spatial determinants of each location, which is the variable with the highest $\varphi(I_u)$ value.

Finally, we compute local interaction effects as the Shapley interaction values do. Shapley interaction values further decompose local effect into main effect and interaction effect. The main effect refers to the individual contribution of each variable, which is independent of other variables and can help us understand the importance of each variable and its impact on the explained variable. The interaction effect considers the synergy between variables. It tells us what kind of impact they have on the

explained variable when multiple variables are considered together. In other words, the interaction effect refers to the additional contribution from the interaction of the variables. The value is calculated as follows:

$$\varphi_{x_i \cap x_j}(I_u) = \left| \sum_{S \in M \setminus \{x_i, x_j\}} \frac{|S|!(|M| - |S| - 2)!}{(|M| - 1)!} (\Delta I_u(S, x_i, x_j)) \right| \tag{8}$$

where, $\varphi_{x_i \cap x_j}(I_u)$ represents the interaction value of the coalition of variables x_i and x_j, $\Delta I_u(S, x_i, x_j)$ represents the additional reward obtained from the coalition:

$$\Delta I_u(S, x_i, x_j) = I_u(S \cup x_i \cup x_j) - I_u(S \cup x_j) - I_u(S \cup x_i) + I_u(S) \tag{9}$$

3. Simulation study

3.1. The design of the simulation study

To evaluate the performance of the GPI model, we conducted three sets of experiments on the simulated dataset (Figure 3). First, we compared the sensitivity of the GPI model and machine learning regression models to the scale of geographic data. Second, we examined the sensitivity of the GPI model to sample size in comparison with regression models. Finally, we benchmarked the GPI model against GWR and Multi-scale Geographically Weighted Regression (MGWR) (Oshan *et al.* 2019).

We designed a synthetic dataset that incorporates different spatial structure. Specifically, we generated two independent spatial predictors X_1 and X_2 over a 50×50 grid, resulting in 2,500 spatial locations. Each predictor was simulated using a spatial random field (SRF) with a Gaussian covariance model, where the mean was set to 1 and the variance to 5, thereby inducing smooth spatial variation across the domain.

The response variable Y was constructed using piecewise-defined functions across three spatial regions (Zone A, B, and C), each representing a distinct generative

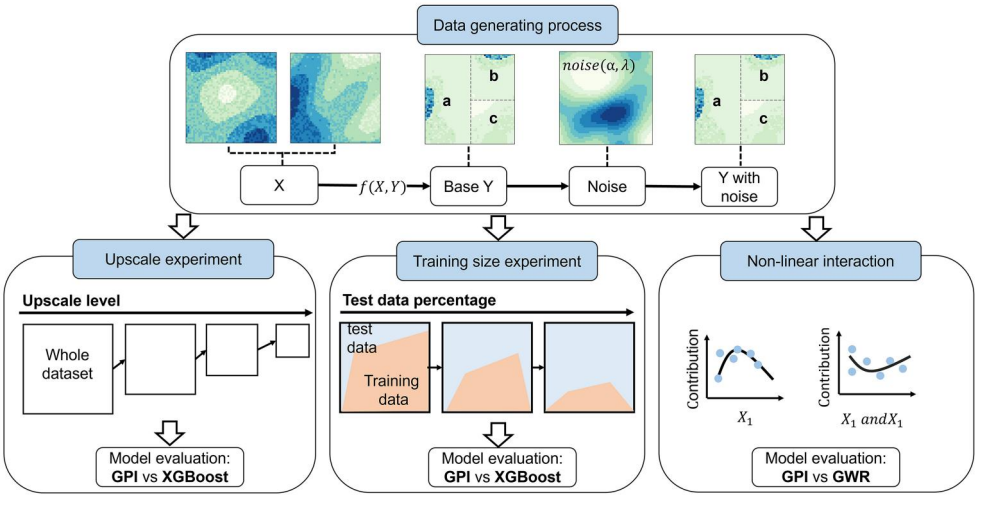

Figure 3. The design of data generating process and three simulation studies.

mechanism and thereby introducing spatial non-stationarity. The spatial domain was further perturbed by adding spatially autocorrelated noise, resulting in the final response formulation:

$$Y_{i,j} = \begin{cases} X_{1_{i,j}} + X_{2_{i,j}}^4 + 2X_{1_{i,j}}X_{2_{i,j}} + \lambda \cdot \varepsilon_{i,j}(\sigma), & \begin{matrix} 0 \le i < 50,\ 0 \le j < 25 \\ (\text{Zone A}) \end{matrix} \\ 2X_{1_{i,j}} + X_{2_{i,j}}^4 + 0.2X_{1_{i,j}}X_{2_{i,j}} + \lambda \cdot \varepsilon_{i,j}(\sigma), & \begin{matrix} 0 \le i < 25,\ 25 \le j < 50 \\ (\text{Zone B}) \end{matrix} \\ 10X_{1_{i,j}} + 0.5X_{2_{i,j}}^4 + 2X_{1_{i,j}}X_{2_{i,j}} + \lambda \cdot \varepsilon_{i,j}(\sigma), & \begin{matrix} 25 \le i < 50,\ 25 \le j < 50 \\ (\text{Zone C}) \end{matrix} \end{cases} \tag{10}$$

In this equation, $\varepsilon_{i,j}(\sigma)$ denotes the spatially autocorrelated noise term. Two parameters are introduced to control the noise properties. The parameter σ defines the standard deviation of the Gaussian kernel used to smooth random noise, effectively determining the level of spatial autocorrelation—the larger the σ, the smoother and more spatially correlated the noise. The parameter λ serves as a scalar weight that controls the overall intensity of the noise added to the deterministic signal. For the first and second simulation experiments, we evaluated the results under different noise levels. Specifically, the values of σ were set to 0.5, 1, 2, 5, and 10, and the values of λ were set to 1, 5, 10, 20, 30, and 100. As a result, for these two simulation experiments, a total of 30 datasets with varying noise levels were generated.

GPI does not involve the construction of regression models, and its interpretation of spatial correlations is expressed through PD values (as is measured by *q* value). In contrast, the confidence of interpretations based on regression methods is constrained by the fitting accuracy of the models. Therefore, in the first and second simulation experiments, we separately calculated the PD values and the coefficient of determination (R^2) for the GPI model and the regression method (XGBoost) to analyze their sensitivity to changes in scale and sample size. The PD value and R^2 are comparable as discussed in a previous study, which established that the PD value is exactly the R^2 of a regression against dummy variables indicating the stratification (Wang *et al.* 2022), enabling a direct comparison between the two metrics. Our simulation experiments were conducted using both Python and R. In the GPI model, we set the min-split parameter to 20 and the complexity parameter (CP) to 0.008 (Luo *et al.* 2022).

3.2. Simulation study 1 – effect of upscaling

In the first simulation experiment, we investigated model robustness across varying spatial resolutions using a block-based aggregation strategy. Specifically, the original 50×50 dataset was downscaled using non-overlapping blocks ranging from 2×2 to 10×10. Within each block, the mean values of predictors and response were computed to produce coarser representations of the data. The two models, GPI and XGBoost, were then applied to the aggregated datasets to assess their ability to capture relationships under different levels of spatial generalization.

Figure 4(a) shows how model performance varies with different spatial smoothness parameters (σ) under fixed noise levels (λ). Each column corresponds to a specific λ, and the rows from top to bottom represent increasing values of σ. A larger σ indicates smoother noise with stronger spatial autocorrelation. Under low noise levels,

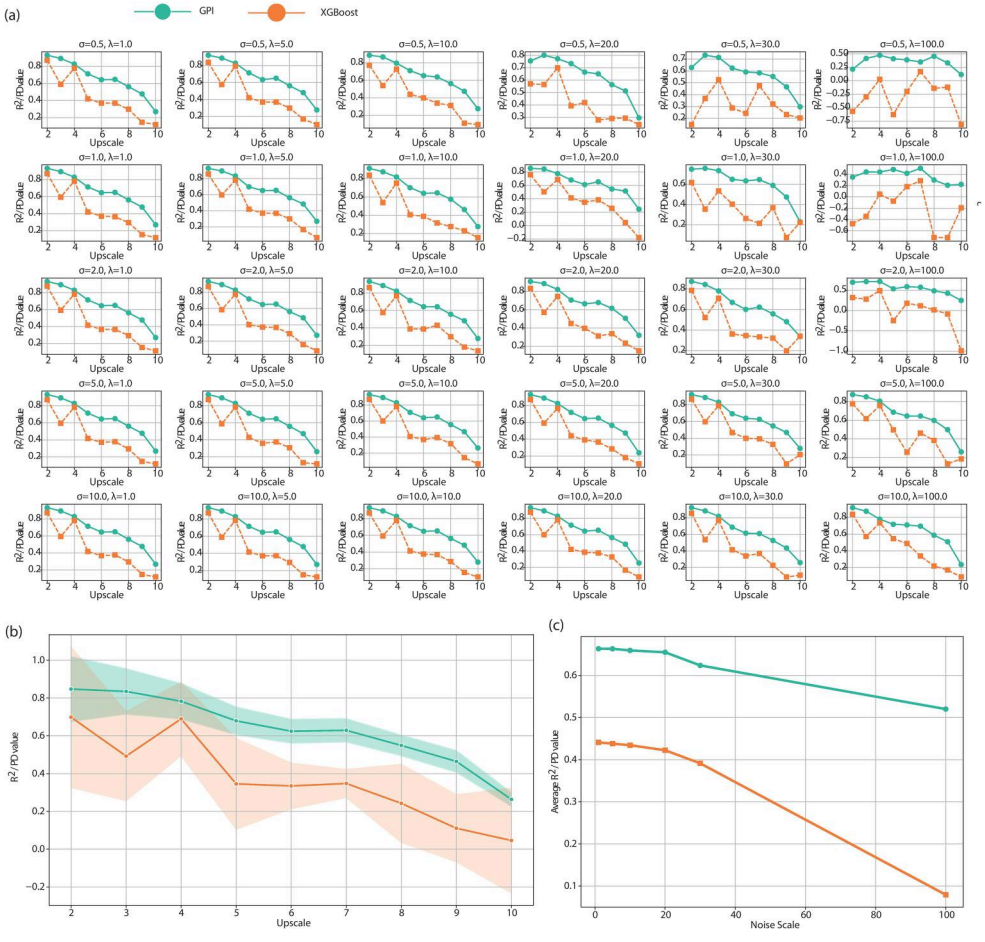

Figure 4. Effect of spatial upscaling on model performance. GPI is shown in green, and the regression-based model (i.e. XGBoost) is shown in orange: (a) model performance across different values of σ and λ under increasing spatial upscaling; (b) aggregated performance across all parameter settings under different upscaling levels; (c) influence of noise scale on model performance.

both GPI and XGBoost exhibit relatively stable performance across different σ values, indicating robustness to spatial noise smoothness. However, at an extremely high noise level (e.g. $\lambda = 100$), both models show improved performance as σ increases. This effect is particularly pronounced for XGBoost. For instance, when σ increases from 0.5 to 10, the PD value of the GPI model improves from approximately 0.5 to 0.8, while the R^2 of XGBoost rises from −0.5 to 0.8. These results suggest that spatially correlated noise, even when large in magnitude, can be better handled by the models—especially XGBoost—compared to highly localized, unstructured noise.

Figure 4(b) summarizes the above results, showing that GPI consistently outperforms XGBoost across all scales and noise conditions, and exhibits greater robustness to changes in spatial resolution.

We further analyzed model performance under different noise levels (λ) in the upscaling experiment (Figure 4(c)). Specifically, we aggregated the scores of each model across varying λ values to examine overall trends. As the noise level increases,

the performance of both GPI and XGBoost declines. However, XGBoost exhibits a much steeper drop, particularly when $\lambda > 20$, indicating its greater sensitivity to high-noise environments compared to GPI.

3.3. Simulation study 2 – effect of training–testing ratio

In the second simulation experiment, we investigated how model performance is affected by limited training data by varying the size of the test set. The total number of samples was fixed at 2,500, and we systematically increased the number of held-out test samples from 1,800 to 2,475—thereby reducing the training set size from 700

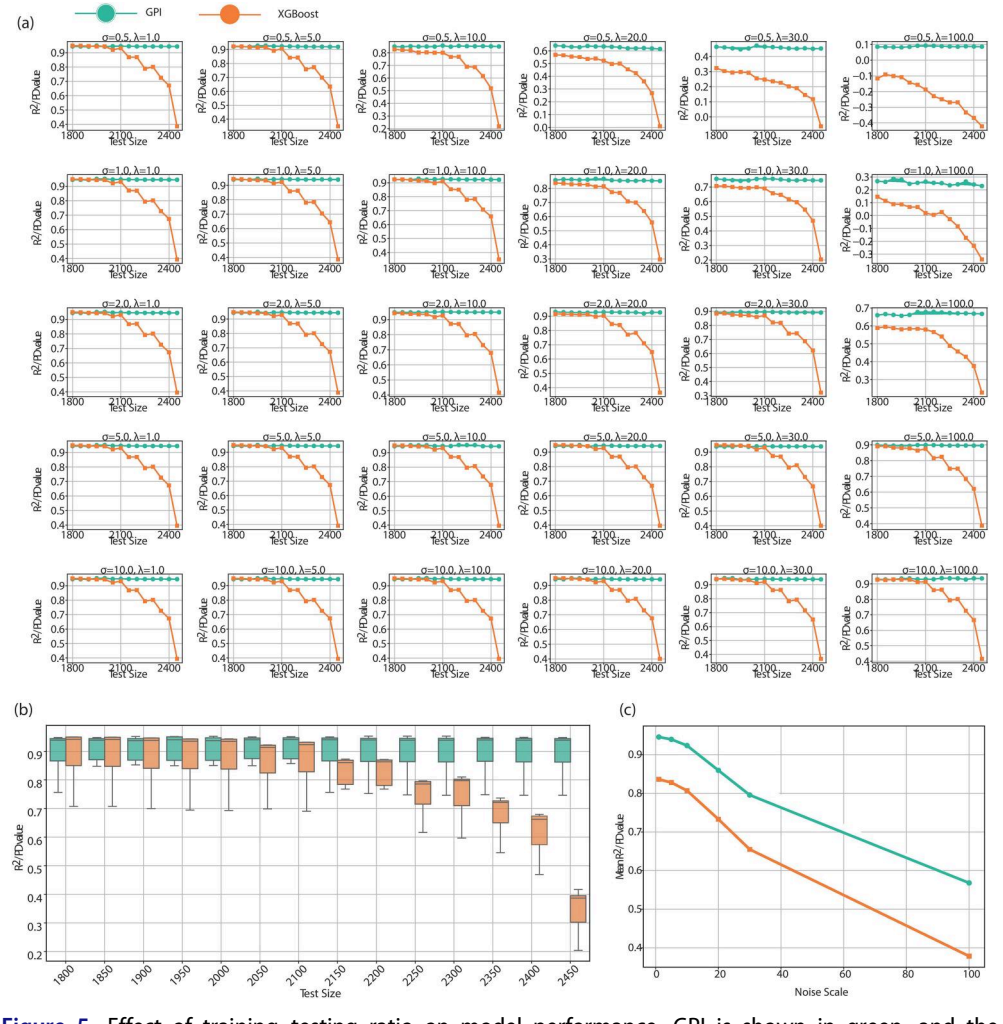

Figure 5. Effect of training–testing ratio on model performance. GPI is shown in green, and the regression-based model (i.e. XGBoost) is shown in orange: (a) model performance across different values of σ and λ as the test size increases (i.e. training set size decreases); (b) aggregated performance across all parameter settings under varying test sizes; (c) influence of noise scale on model performance.

to just 25. Both GPI and XGBoost were trained on the remaining data and evaluated on the held-out test sets.

As shown in Figure 5(a,b), XGBoost exhibits substantial sensitivity to the amount of training data, with performance deteriorating rapidly as the training size decreases (i.e. when the test set exceeds 2,000 samples). In contrast, GPI maintains relatively stable PD values, demonstrating stronger robustness across a wide range of data availability conditions. This pattern holds consistently across different noise levels and spatial autocorrelation parameters (λ and σ).

As is shown in Figure 5(c), consistent with the findings from the first simulation study, we observe that under high noise levels (e.g. $\lambda = 20, 30, 100$), the spatial autocorrelation of noise—controlled by the smoothness parameter σ—has a substantial impact on model performance. For instance, at $\lambda = 100$, when $\sigma = 0.5$, the PD value of the GPI model is only around 0.1. However, when σ increases to 10, the PD value dramatically improves to approximately 0.9. This highlights the importance of spatial structure in mitigating the negative effects of high-magnitude noise.

The above findings regarding the effect of the training–testing ratio highlight a critical limitation of regression-based explainable AI models: when training data is limited, models such as XGBoost may produce highly unstable and unreliable explanations. In contrast, GPI provides scale-robust and consistent interpretability, even under severe data scarcity.

3.4. Simulation study 3-nonlinear interaction

In the last experiment, we applied the GPI, GWR, and mGWR models on simulated data to explore the relationship between the variables. For the GWR and mGWR model, we employed the mgwr Python package. The bandwidth selection was performed using the default adaptive bi-square kernel function, with the optimal bandwidth automatically determined by the bandwidth selection module in the mgwr package. As shown in Figure 6, the first to third rows present scatter plots of X_1, X_2, and $X_1 * X_2$ against the corresponding predicted values in the three models: GPI, GWR, and mGWR, respectively. The GPI model can capture the nonlinear interaction effects between variables, as calculated by Equation (8). As shown, the strongest interaction effect reaches a value of 125, occurring when the product of X_1 and X_2 is close to zero. In contrast, GWR and mGWR are unable to account for nonlinearities and are prone to misinterpreting nonlinear relationships as spatial variation effects (Sachdeva *et al.* 2022; Li *et al.* 2023).

4. Case study: Identifying factors influencing the risk of homelessness based on GPI

4.1. Study area and data

We implemented our model to explore the spatial associations in homelessness risk data from Australia in 2016 (Parkinson *et al.* 2019). The data were from Australian Bureau of Statistics, recording the number of people at risk of homelessness per 10,000 at the Statistical Area Level 3 (SA3) level (Australian Bureau of Statistics 2016). The risk indicator of homelessness represents the percentage of the population lacking a permanent residence, compelled to dwell in open spaces, temporary shelters, or

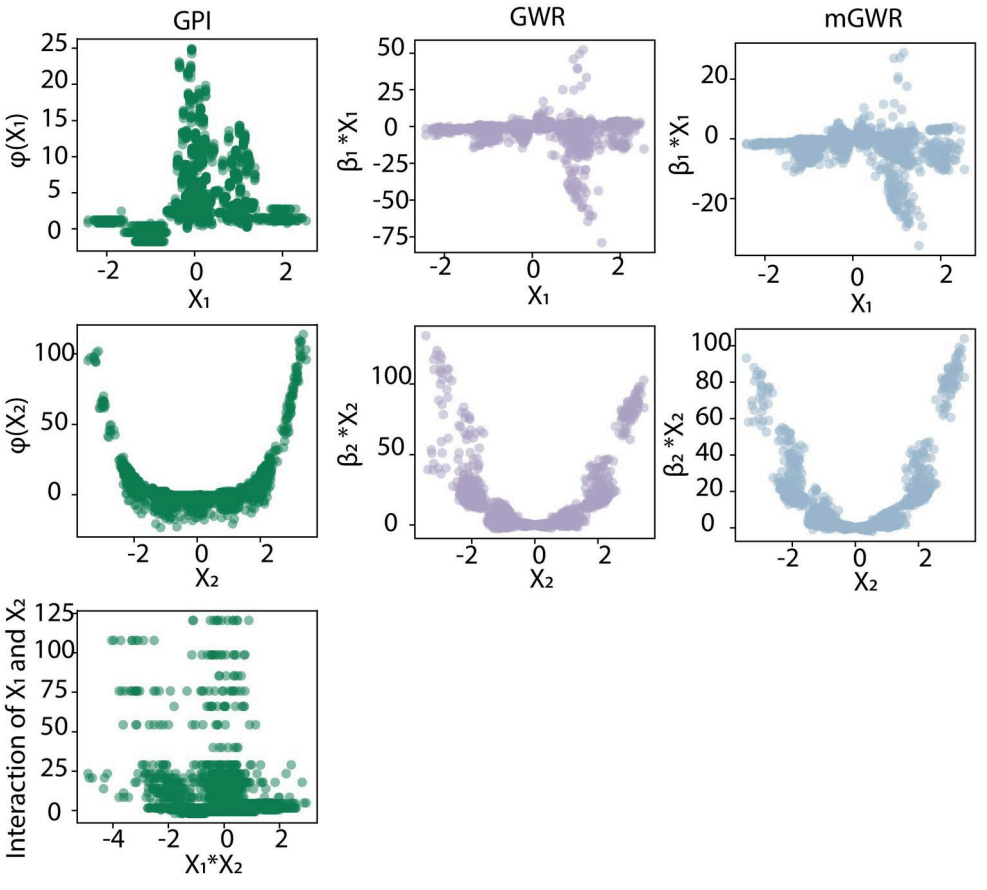

Figure 6. Capturing nonlinear interactions among variables using GPI model.

inadequate living conditions. This metric is widely employed to evaluate the socio-economic circumstances and fairness within a country or region. Individuals who lose stable housing often encounter challenges such as diminished employment prospects and increased health problems, ultimately resulting in increased social security expenditures and economic burdens. Comprehending and addressing the risk of homelessness is an essential step toward a just and compassionate society in Australia. By reducing this risk, we can foster greater social integration, thereby promoting social harmony (Caton *et al.* 2005). A precise understanding of the extent and causes of homelessness empowers the government to formulate more effective social policies and intervention strategies to help those most in need.

Figure 7 shows the spatial distribution of homelessness risk in Australia. The homeless risk is high in the central and northern regions, whereas low in the eastern and western coastal regions. It has an evident spatial heterogeneity inside several major cities, which is high in the city centers and nearby suburbs.

For the analysis of the spatial association, data of seven socio-economic indicators were collected as the explanatory variables that are potentially related to the homelessness risk. They are population size, population density, unemployment rate,

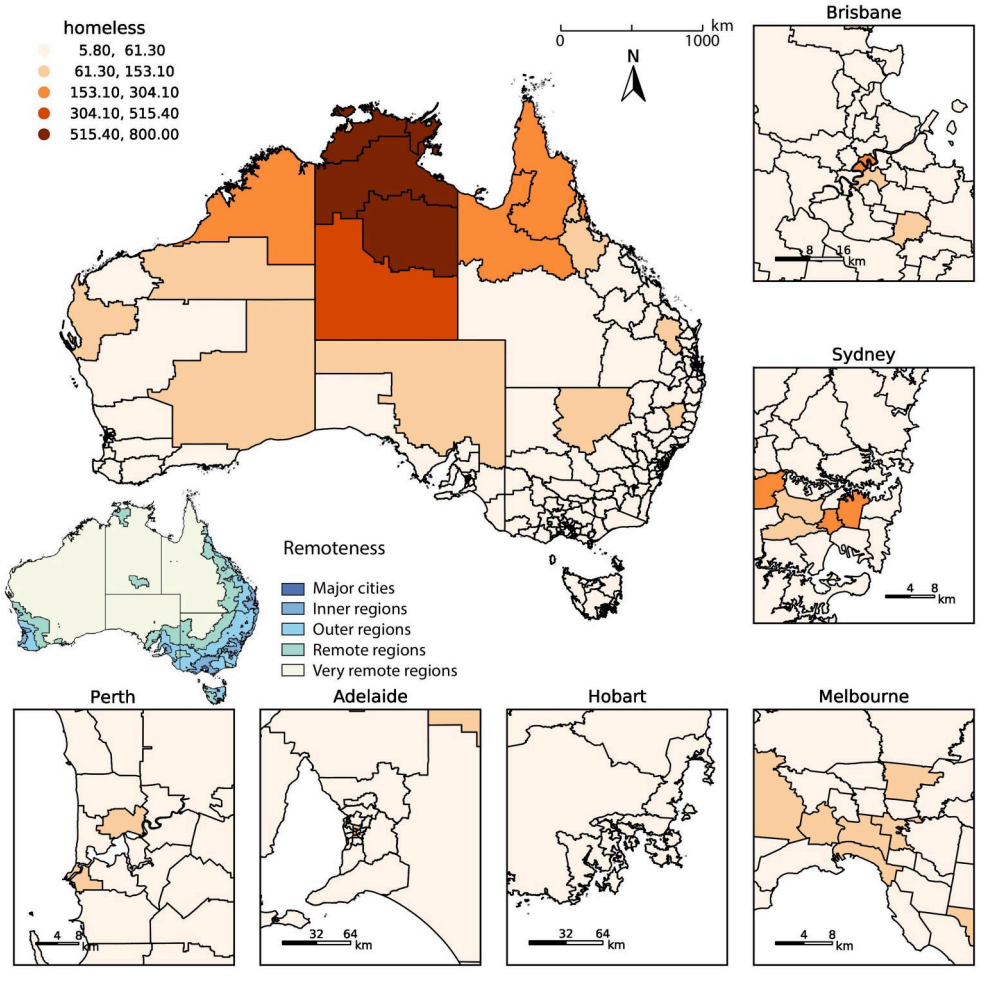

Figure 7. The spatial distribution of homeless risk in Australia. The small map displays the remoteness classification of Australia.

proportion of dwellings without internet connection, rental costs, mortgage rate, and commuting distance to work. All variables were collected at the SA3 level (Table 1).

4.2. The workflow of applying GPI for the case study

The proposed GPI model was employed to investigate the factors associated with the homelessness risk in Australia. First, we conduct data preprocessing and generate the geographical pattern interaction. The distribution of the homelessness risk in Australia was divided into several subzones based on the interaction among explanatory variables. This geographically optimized zoning forms the basis for our subsequent analysis using the GPI model. Second, we assessed the global univariate effects in GPI, calculating the spatial association of individual variable with the homelessness risk. Third, we evaluated the local univariate effects in GPI. The spatial locally impact of each individual variable on homelessness risk was estimated. Finally, to validate the model's

performance and robustness, a sensitivity analysis was conducted using the leave-one-out method. In this approach, we systematically removed one region at a time from the model's input data and examined the resultant changes in dominant variables. The model sensitivity was gauged by measuring the percentage change in these dominant variables across each region.

5. Results

5.1. The clustering pattern of homelessness-related variables

Figure 8 depicts the optimal geographic zones of homeless risk in Australia, determined by seven explanatory variables. Five distinct sub-zones with homogeneous homelessness risk were identified. Zone A, having the lowest homelessness risk with an average value of 32.7, primarily comprises eastern cities. Zone B, mainly located in the eastern coastal regions, has a slightly higher average homelessness risk of 58.8 than Zone A and the highest average unemployment rate among the five zones at 9.8%. Zone C encompasses most of the vast western inland areas, and also includes

Table 1. Explanatory variables of the homelessness risk.

Name	Code	Description
Population	pop	Estimated resident population
Population density	popdens	Population density (persons/km^2)
Unemployment rate	unemployment	Unemployment rate (%)
Non internet rate	noninternet	Proportion of dwelling without Internet access (%)
Rental payment	rentalpay	Median weekly household rental payment ($)
Mortgage affordability	affordmort	Households where mortgage repayments are more than 30% of imputed house hold income
Distance to work	diswork	Average commuting distance from place of usual residence to work (km)

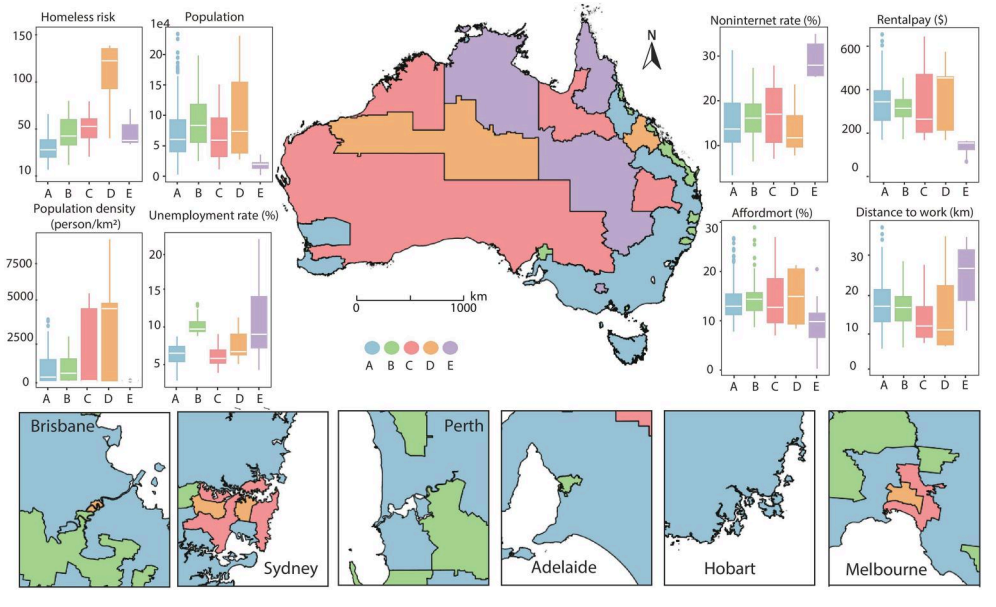

Figure 8. The geographical pattern interaction: geographically optimal zones of homelessness risk.

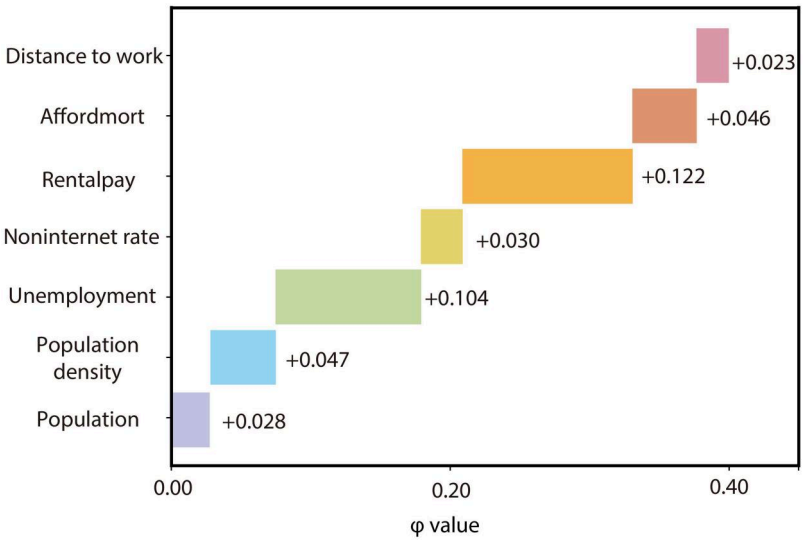

Figure 9. Global univariate effects in GPI, illustrating the overall contribution of individual variables to homelessness across the entire spatial domain (i.e. Australia).

some regions in major cities like Sydney and Melbourne. Zone D, with the most severe homelessness problem (average risk of 206.2), includes several inner areas and inner cities of Sydney and Melbourne. Zone E, characterized by a sparse population (average population density of 0.9), has the highest average non-internet rate (29.1%) and distance to work (24.2 km), as well as the lowest average rental payment (128.9$) and mortgage affordability (9.1%).

5.2. Global univariate effects in GPI

Figure 9 illustrates the strength of the correlations between individual variables and the homelessness risk. The interaction of seven explanatory variables explain totally 40% of the spatial disparities of homelessness risk. Among them, rental payment has the strongest association, with a φ value of 0.122. Next is unemployment rate, which can explain 10.4% of the homelessness risk. High rental costs may reduce the affordability of some individuals to housing expenses, forcing them to become homeless. Therefore, rental payment is likely a contributing factor to the increase of the homelessness risk. Similarly, as the unemployment rate rises, more people may lose their jobs, struggle to sustain their livelihoods, and face the risk of homelessness. Hence, an increase in the unemployment rate might lead to a rise in the homelessness risk.

The associations between population density, mortgage affordability, the rate of no internet, and the homelessness risk are similar, with φ values of 0.047, 0.046, and 0.030, respectively. Poorer mortgage affordability could be associated with a higher risk. If some individuals are unable to pay their mortgages, they may lose homeownership. Higher population density refers to a greater number of people residing in a given area. Areas with higher population density may be more susceptible to experiencing a higher homelessness risk. This could be due to increased competition for limited housing resources and higher rental costs, making it difficult for some individuals

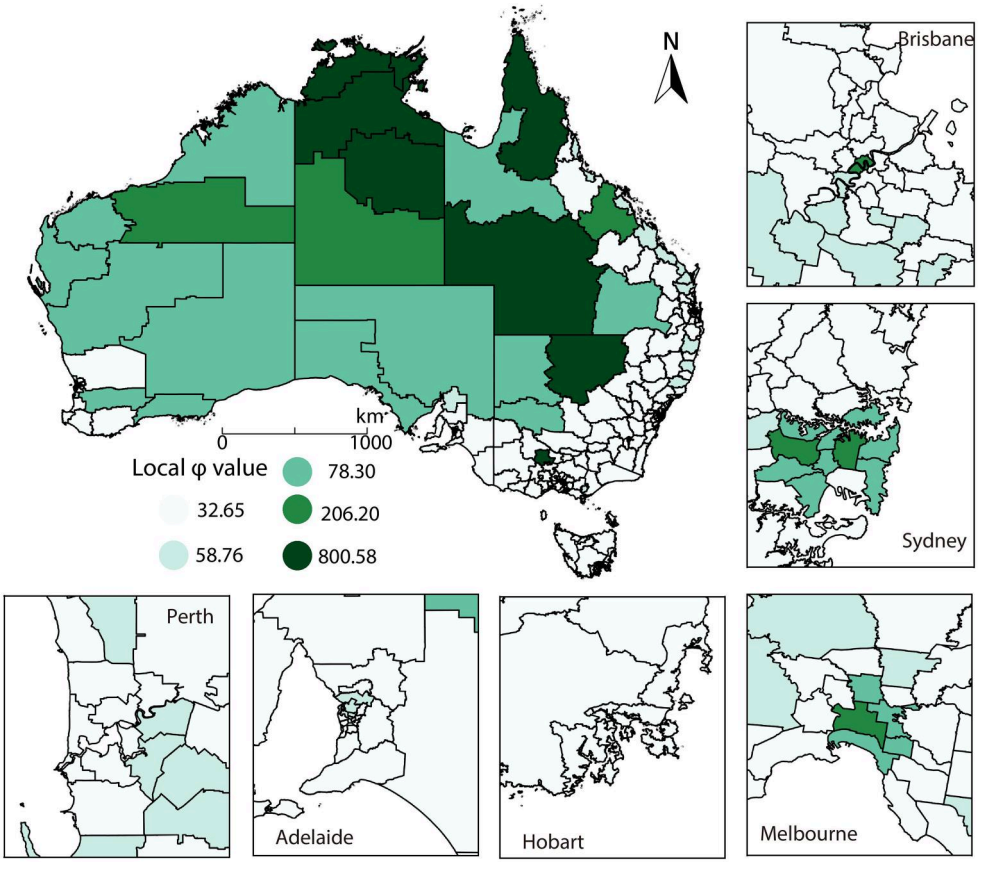

Figure 10. Local effects in GPI, representing the overall contribution of all explanatory variables to homelessness at each location.

to afford housing. The lack of internet access could be related to the homelessness risk by preventing individuals from accessing job information, educational resources, and social assistance, thereby increasing the homelessness risk.

5.3. Local univariate effects in GPI

5.3.1. Local effects of GPI

Figure 10 shows the local effects of GPI among all explanatory variables. The spatial distribution of explanatory variables exhibit a significant clustering pattern in their local effect on homelessness risk. The Moran's I is 0.35, with a Z score of 9.78. The local effect in most southeast coastal regions is relatively low (32.65), while its considerably high (206.20) in the city centers of Sydney, Melbourne, and Brisbane. This reveals a strong association between explanatory variables and homelessness risk in the major urban areas.

5.3.2. Local univariate contributions

Figure 11 shows the local univariate contribution of each explanatory variables. In coastal and urban areas (major cities, inner, outer regions), population may be a

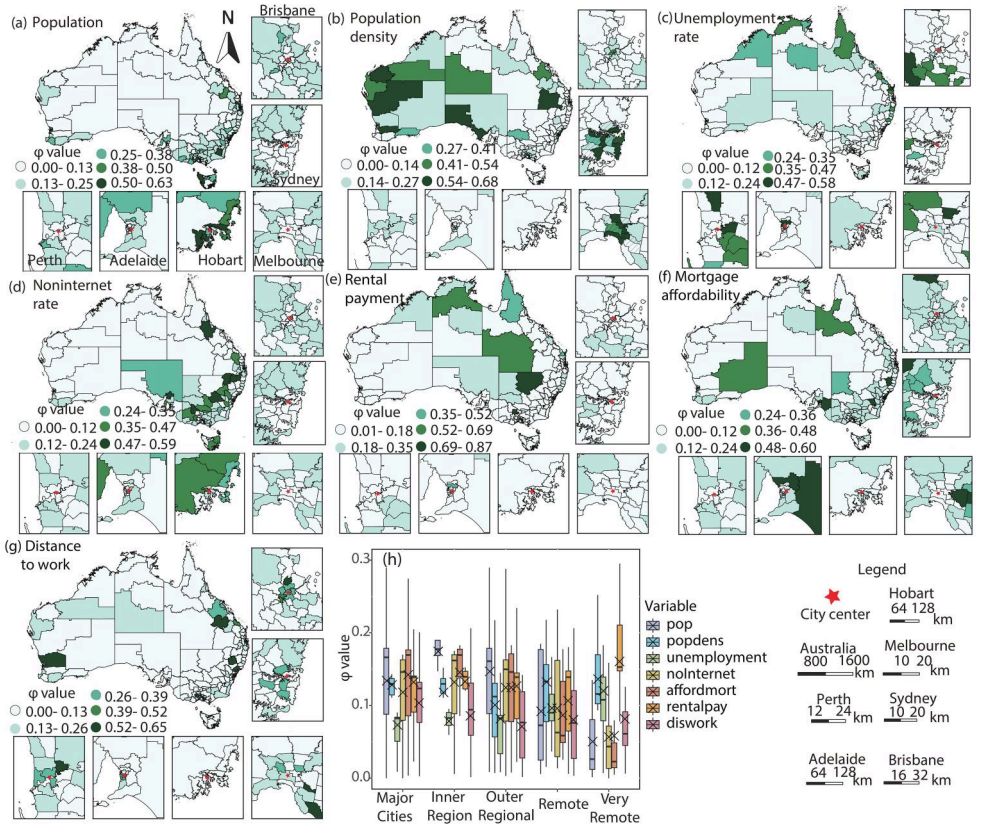

Figure 11. The local univariate effects in GPI: (a) Population; (b) population density; (c) unemployment rate; (d) non-internet rate; (e) rental payment; (f) mortgage affordability; (g) distance to work.

primary factor contributing to homelessness risk since population influences housing demand. In addition, the mortgage affordability plays a crucial role because the high cost of homeownership can exert financial pressure on low-income households, thereby increasing homelessness risk. In inland and remote areas (remote, very remote), population density and the proportion of rental payments are more closely associated with the homeless risk. Population density can be related to the balance between housing supply and demand, and in areas with lower population density, it may be challenging to provide an adequate range of housing choices. In these regions, the burden of high rental payments can significantly affect the economic stability of low-income households. Due to limited opportunities for homeownership, many individuals may rely on renting, and high rental costs can lead to financial instability, thereby increasing the risk of homelessness.

5.3.3. Non-linear pattern of contributions

Figure 12 indicate the non-linear contributions of explanatory variable values to the risk of homelessness. Figure 12 (a) reveals relationship between the population and its contribution to homelessness risk. For areas with a smaller population, population size

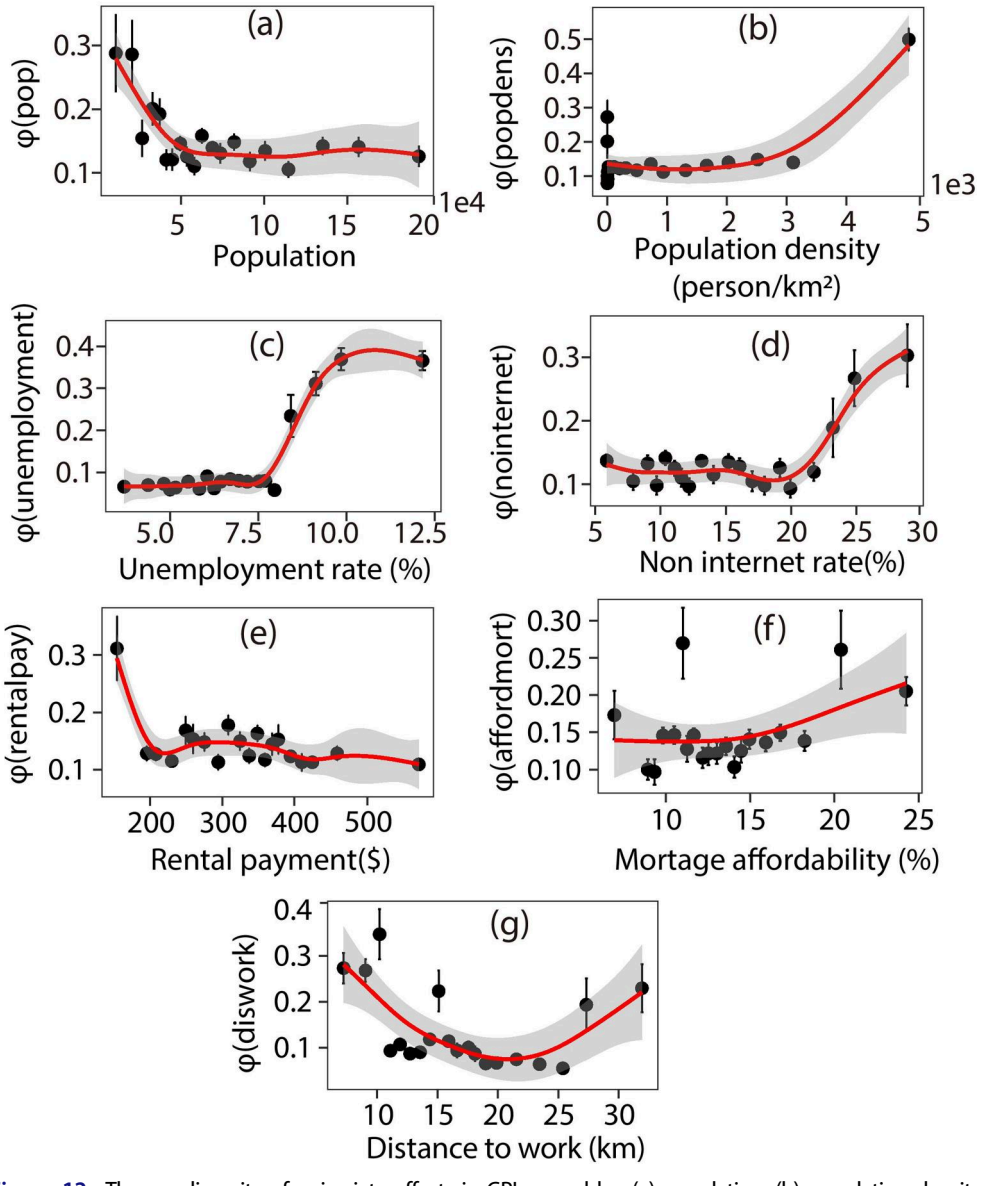

Figure 12. The non-linearity of univariate effects in GPI caused by: (a) population; (b) population density; (c) unemployment rate; (d) noninternet; (e) rental payment; (f) mortgage affordability; (g) diswork.

significantly influences the homelessness risk. However, as the population increases, this correlation diminishes. Below 50,000 in population, a strong association exists, but above this threshold, the correlation stabilizes at a lower level. This suggests that beyond a population of around 50,000, community complexity and diversity increase, leading to the saturation of the population's impact on the homelessness risk. The unemployment rate (Figure 12(c)) and the rate of no internet (Figure 11(d)) have similar effects on homelessness. A rising unemployment rate ($>$ 7.5%) and lack of internet access ($>$ 20%) significantly increase homelessness risk, contributing around 40% and 30%, respectively. These effects reflect economic instability, where job loss and limited

digital access hinder employment opportunities, triggering housing insecurity. The abrupt shifts at these thresholds highlight the non-linear nature of economic systems, where downturns and feedback loops exacerbate homelessness. Figure 12(e) shows that rental payments strongly impact homelessness risk in low-rent areas, but this effect weakens as rents rise (>200 units). Higher rents do not necessarily increase homelessness, but low-income households remain highly vulnerable to rent hikes. This highlights the need for region-specific policies, such as housing subsidies or rent controls, to mitigate financial strain on low-income groups. Figure 12(g) shows an inverted U-shaped relationship between commuting distance and homelessness risk. Short (<10 km) and long (>25 km) commutes correlate with higher risk, while intermediate distances show weaker associations. In city centers, high housing costs may force low-income individuals into homelessness. Conversely, those in distant suburbs face financial strain from long commutes and transportation costs, increasing their vulnerability to homelessness.

5.3.4. Spatial determinants of homelessness risk

Figure 13 shows the spatial determinant of homelessness risk in Australia, which is the explanatory variable with the strongest association with homelessness risk in each

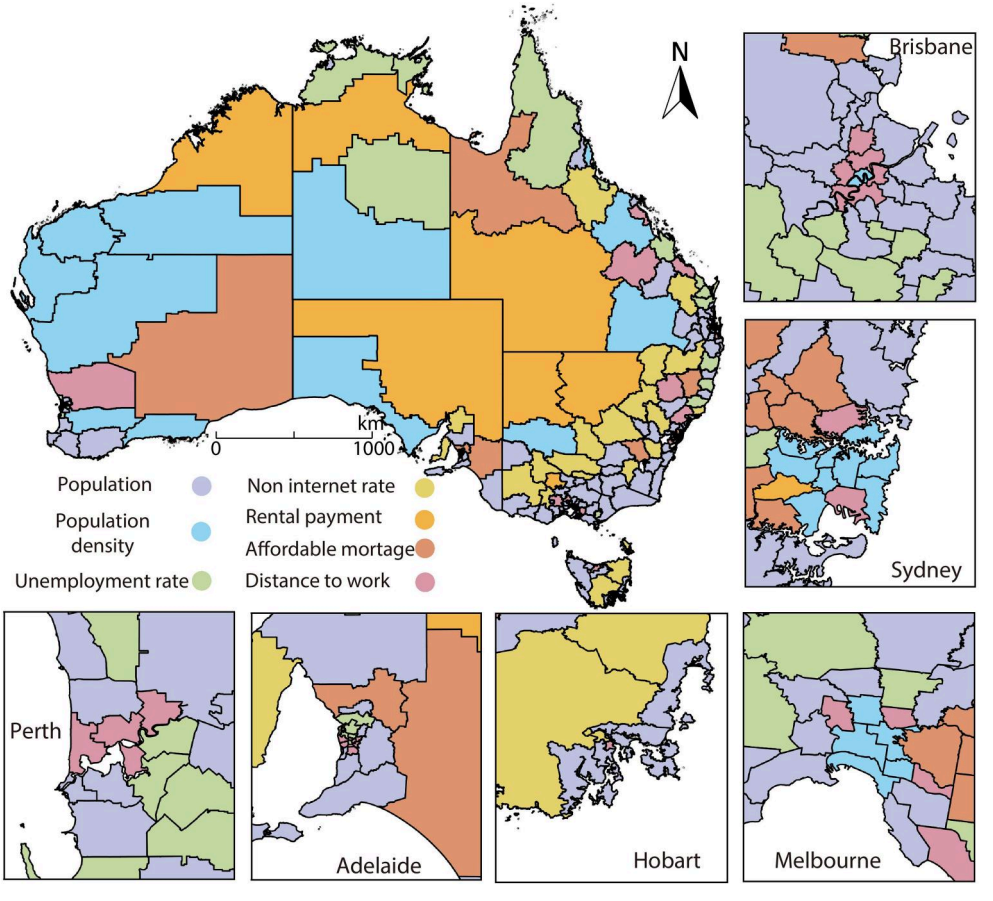

Figure 13. The spatial dominants of the homelessness risk in GPI at each location, which represent the variables that have the strongest association with the homelessness risk.

location. Regarding three major cities, Sydney, Melbourne, and Brisbane, the most significant variables associated with homelessness risk are found to be pop density, population, and distance to work. The results show a similar spatial pattern in three cities: from the city center to the suburbs, the most influential variables associated with homelessness risk are changing from popden, diswork, and pop, respectively. This indicates that in the central areas of large metropolises, population density has the strongest correlation with homelessness risk. In the outer city areas, the number of homelessness individuals is more closely related to commuting distance. In urban suburbs, population size plays a crucial role concerning homelessness risk. Regarding three smaller cities, Perth, Adelaide, and Hobart, a different spatial pattern is observed. In the central areas of these cities, commuting distance has the most significant impact on homelessness risk. In other areas and suburbs of the cities, the variables with the strongest association with homelessness risk are population density and population size.

5.3.5. Local bi-variate effects in GPI

Figure 14 shows the interaction matrix in six major cities, which describes the interaction effects between each pair of variables to homeless risk. The larger the value, the stronger the interaction between the variables, and the greater the impact on the homeless group. Interaction between rental payment and other variables has an important impact on homelessness risk. The spatial heterogeneity of the interaction of variables can be perceived in the heatmap. The interaction between rental payment and population density has significant impacts on homelessness risk, particularly in major cities such as Sydney, Melbourne, and Brisbane. Higher rental payment coupled with elevated population density exacerbates the risk of homelessness. The intensified demand for housing in densely populated areas amplifies rental costs, placing a

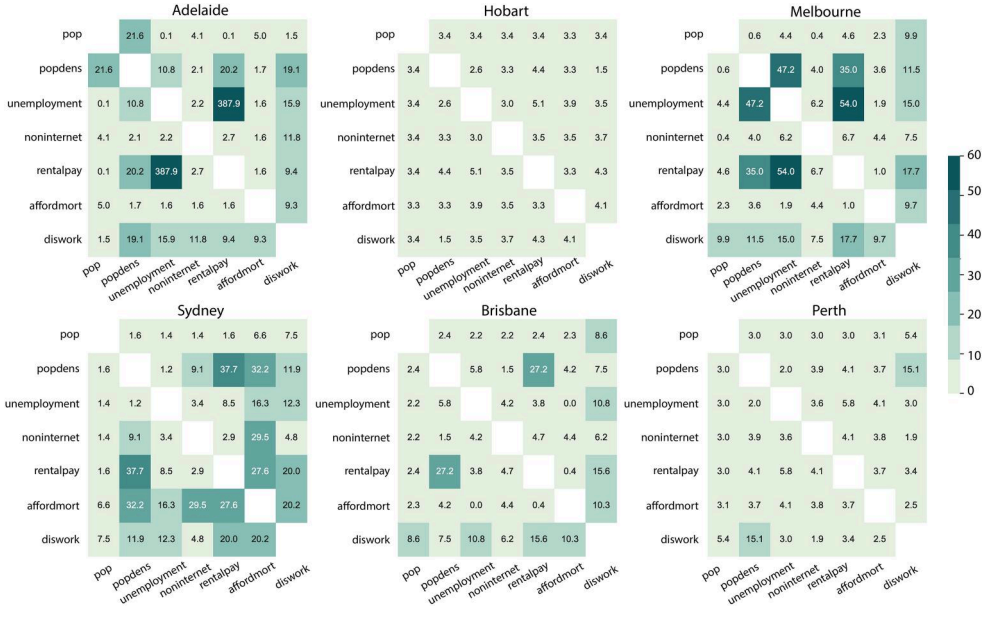

Figure 14. The local interaction effect in GPI.

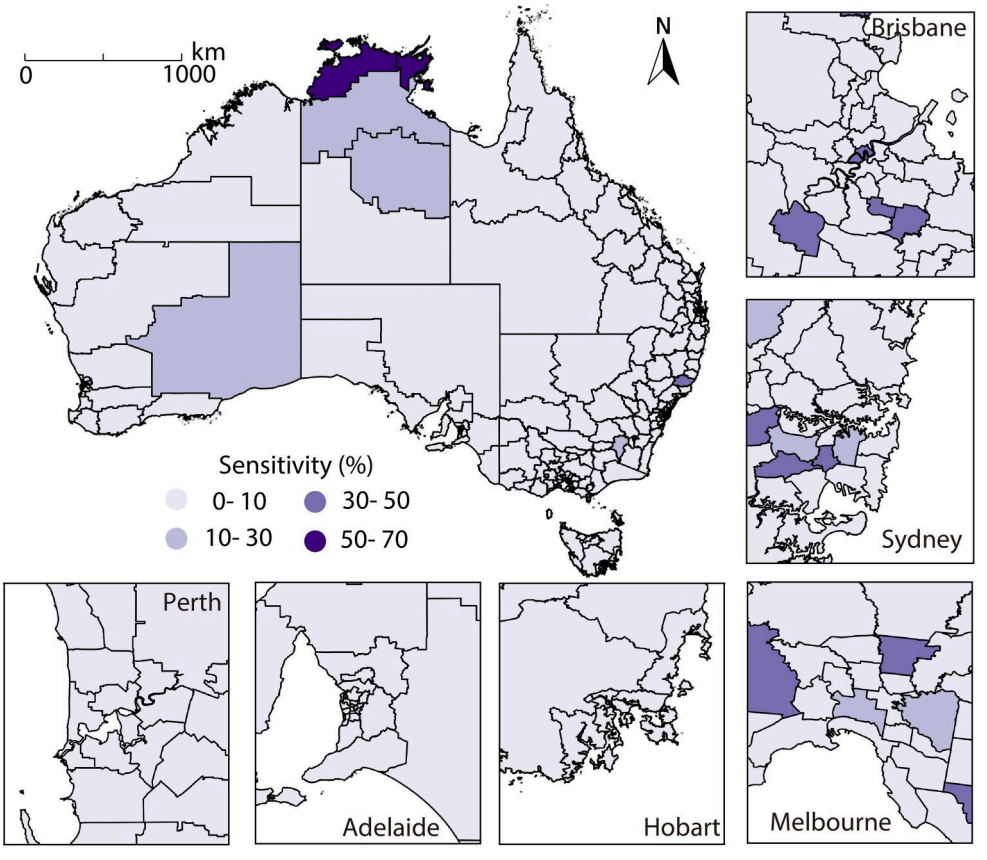

Figure 15. The sensitivity analysis of GPI model. The value refer to the percentage change in the dominant variables when this region is excluded from the model's input data.

disproportionate burden on individuals and families with limited financial resources. In Sydney, Melbourne, and Brisbane, where population density is relatively high, the cost of housing tends to surge due to the demand-supply dynamics. As a result, the convergence of high rents and dense population further marginalizes economically disadvantaged individuals and households, making them vulnerable to homelessness. Moreover, the competitive housing market in densely populated urban areas can limit access to affordable housing options, further exacerbating the homelessness risk.

5.4. Model validation

In the study, GPI model is validated through a sensitivity analysis (Figure 15). In 90% of the regions, the percentage change in the dominant variables is below 10%, indicating the robustness of our model. The dominant variables exhibiting notable variations primarily concentrate in northern Australia, an area concurrently characterized by a relatively high homelessness risk. This may be because that the GPI model relies on decision tree algorithm for the spatially optimized discretization of the homelessness risk, which tends to exhibit sensitivity to outliers to a certain extent.

6. Discussion

6.1. The advantage of using spatial pattern to explain geographical interactions

Previous models for analyzing the association of geographical variables are limited in exploring the non-linearity of relationships and interactions between multiple variables. First, they often assume linear relationships between variables, whereas, in reality, the relationships between geographical variables are often complex and nonlinear (Zhu *et al.* 2022). This leads to the existing models needing improvements to capture the relationships among geographical phenomena accurately. Second, existing models require to pay more attention to the spatial interactions between geographical variables. This study proposes the GPI model that uses spatial patterns to characterize geographical variables' spatial dependence and spatial heterogeneity for exploring spatial association. By discretizing the geographical space and analyzing the variance and mean of response variables for different strata, the GPI model can better describe the characteristics and patterns of geographical phenomena at different locations, providing more accurate identification of spatial relationships.

The GPI model is based on two fundamental statistical indicators, variance and mean, to characterize spatial patterns and to describe heterogeneity and stationarity, respectively. Variance is a statistical measure of data dispersion, indicating the degree of difference between data points and their mean. A higher variance implies greater differences between data points, representing significant global stratified characteristics. Thus, variance describes global stratified features, i.e. differences between different groupings. In our model, by calculating the between-group variance of response variables for different grouping methods, we can assess the contribution of each explanatory variable to the global stratified features. When a specific explanatory variable contributes significantly to the global stratified features, the corresponding grouping method will lead to a higher between-group variance, reflecting the importance and impact of that explanatory variable. Mean is a statistical measure of the central tendency of data, representing the average position of data points around the average value. In our algorithm, we can describe the local stationary features at each location or region by calculating the within-group mean of response variables for each grouping method. When a specific explanatory variable contributes significantly to the local stationary features, the corresponding grouping method will significantly change the within-group mean at that location. Thus, the within-group mean for each location or region can express local stationary features. This study introduces the interpretable machine learning algorithm Shapley to detect the contribution of individual variables in the interaction of multiple explanatory variables. Therefore, the GPI model can effectively identify each variable's contribution to the relationships among geographical phenomena with the consideration of their spatial interactions and provides a more comprehensive explanation of the correlations between geographical variables.

6.2. The differences between the GPI model, SSH models, and regression-based XAI methods

In this section, we first discuss the differences between the GPI model and SSH models, with a particular focus on the improvements introduced by GPI. We then analyze

the distinctions between the GPI model and currently popular spatial XAI methods, which are primarily designed to explain the outputs of machine learning prediction models.

The GPI model is an innovative algorithm for analyzing spatial relationships based on the similarity of spatial distributions, with its core concepts motivated by SSH models for modeling discrete spatial heterogeneity. Therefore, it is crucial to compare the differences between the GPI model and previous SSH models. Consider a task that aims to explore the relationship between three explanatory variables and a dependent variable *Y*. The initial SSH model, geographical detector (Wang *et al.* 2010), employed basic spatial discretization methods, such as quantiles, which did not consider that different variables may require distinct grouping strategies. This limitation often led to underestimating the spatial relationships. To address this issue, the GOZH model was introduced to enhance the spatial discretization process. It utilized decision tree algorithms to group *Y* based on the values of explanatory variables *X*, allowing for more precise identification of spatial relationships. However, GOZH was limited in two key aspects. First, it could only calculate the overall correlation between multiple explanatory variables and *Y* without disentangling the individual contributions of each variable. Second, it was unable to capture spatially varying relationships. In response to these limitations, the GPI model was developed to account for both interaction effects and spatially varying relationships, providing a more comprehensive framework for spatial analysis.

Based on our simulation results, we further clarify the conceptual differences between the GPI model and existing spatial XAI methods. While GPI can be combined with many XAI techniques, such as SHAP, GeoShapley, and LIME, it proposes a fundamentally different framework for geographic interpretation. Current spatial XAI approaches primarily explain the outputs of trained prediction models (e.g. statistical or machine learning models), whereas GPI directly analyzes the spatial distributions of variables without relying on predictive modeling. As a result, GPI represents a different paradigm. Spatial regression-based XAI methods, including the combination of XGBoost with SHAP as well as more recent frameworks like GeoShapley (Li *et al.* 2023) and XGeoML (Liu 2024), rely heavily on the predictive performance of underlying machine learning models. This dependence introduces inherent limitations, affecting both the generalizability and the reliability of their interpretative outputs.

First, when the prediction model fails to fit the data effectively, the credibility of the spatial XAI outputs diminishes substantially. Although spatial XAI outputs quantify the contributions of individual features to model outputs, they primarily reflect the internal mechanisms of the trained model rather than the true underlying spatial relationships. In cases where model fitting is poor, even seemingly reasonable explanations can deviate significantly from actual geographic reality. This issue is particularly acute in geospatial applications, where datasets are often sparse and unevenly distributed, limiting the model's ability to capture complex spatial patterns and increasing the risk of overfitting.

Second, spatial XAI methods lack robustness across regions and scales. Geographic feature relationships can vary considerably between areas, and prediction models that perform well locally may fail when applied elsewhere, reducing the transferability and

consistency of interpretations. In contrast, the GPI model does not require model fitting or retraining across regions. Instead, it consistently applies a spatial partitioning and correlation analysis framework, enhancing generalizability without being dependent on local model performance.

Third, regression-based approaches are sensitive to variations in sample size and variable selection, leading to instability in feature attribution outcomes. This instability is particularly problematic in geographic contexts, where spatial scale issues such as the Modifiable Areal Unit Problem (MAUP) further complicate model interpretation. In contrast, GPI captures intrinsic spatial structures directly from data without fitting predictive models, providing greater robustness across different spatial scales and sample densities.

The advantages of the GPI model over other spatial explanation methods are summarized as follows:

- **Independence from model fitting**: Unlike regression-based XAI methods that rely on training statistical or machine learning models, GPI derives interpretable results directly from the spatial distributions of variables without requiring predictive modeling. This independence enhances both the robustness and reliability of GPI's interpretations.
- **Explicit spatial interpretability**: GPI explicitly constructs spatial discretizations through decision trees and computes Shapley values across partitioning outcomes to quantify variable contributions. This structure enables clear visualization of how features interact across space. In contrast, explanations derived from machine learning regression models remain constrained by the black-box nature of those models, making the spatial decision-making processes less transparent.
- **Adaptability to spatially stratified heterogeneity**: In regression-based XAI models, the importance of a variable is typically interpreted based on the continuous marginal influence of X on Y. By contrast, GPI evaluates the effect of adding or removing a variable X on the spatial distribution of Y, allowing for abrupt, discontinuous changes. This computational framework effectively captures spatial relationships under stratified heterogeneity, where traditional smoothness assumptions often fail, especially over large and complex geographic surfaces.
- **Robust performance across different spatial scales and sample sizes**: Compared to traditional spatial regression models, SSH models, and regression-based spatial XAI methods, GPI maintains stable interpretive performance across varying spatial resolutions and extents. In addition, GPI consistently provides reliable results under limited sample conditions, effectively avoiding the overfitting issues commonly observed in prediction-based methods.

6.3. Limitations and future works

There are still some limitations to this study, and a few future works are recommended. For instance, it is recommended to systematically assess the relationship between the GPI model and existing spatial regression methods. These models have inherent methodological differences, making direct comparisons challenging. In

existing spatial regression models, coefficients represent the strength of interaction between independent and dependent variables. For example, in the GWR model, the coefficient represents the impact of a unit change in the independent variable on the dependent variable within a specific geographical area. The proposed GPI model is not constrained by the linearity of relationships but quantifies interaction strength by considering the spatial distribution patterns of geographic variables. We identified an inherent connection between GPI and traditional spatial regression. In GPI, the influence of independent variables on the dependent variable depends on the extent to which their consideration affects the spatial distribution, similar to the concept of coefficients in traditional spatial regression methods. However, there are still paradigmatic differences between GPI and existing spatial regression methods, making mutual validation challenging. In existing spatial regression, the relationships between geographic variables are often characterized by a polynomial function, while GPI, based on pattern interaction, resembles more of decision rules (Apté and Weiss 1997). The advantage of decision rules is their ability to describe discontinuous spatial relationships, where the impact between geographic variables exhibits abrupt, non-continuous changes. In future research, we will discuss the more fundamental connections between GPI and existing spatial regression methods, enabling the design of rational simulation experiments for meaningful inter-method comparisons.

The second limitation is the univariate effects cannot indicate the direction of the association. When calculating the global univariate effects (Equation 4), we considered the presence or absence of variables in the GOZH model and adopted the concept of Shapley values. Typically, adding an explanatory variable in the GOZH model leads to a positive contribution to the outcome. As a result, the univariate effects are usually positive and cannot indicate the direction of variable relationships. In future studies, we will explore methodological advancements to integrate directional effects into the model. In addition, the GPI model incorporates spatial correlation analysis. A potential direction for future research is to explore causal inference within the GPI framework. For instance, by considering the similarity of the spatial patterns of two variables from the time series data, we could evaluate their causal relationship.

In addition, it should be noted that when the GPI model leverages SSH to explain global spatial relationships, there may be a potential risk of overestimating variable contributions in datasets with high spatial autocorrelation. In addition, since GPI relies on CART for spatial partitioning, the number and structure of the partitions may also influence the results. Future research could explore more robust partitioning methods that are better suited for highly spatially autocorrelated data.

Third, endogeneity is an issue that requires attention in future research. In the GPI model, we capture and understand the spatial interactions between variables by analyzing the similarity of their spatial distributions. Compared to traditional regression-based statistical methods, this approach reflects spatial associations between variables more directly, making it more reliable for handling spatial data and reducing the impact of endogeneity. However, it is also acknowledged that, even in non-regression models, spatially autocorrelated errors can impact the reliability of relationships between variables. To address this, future research will explore the integration of spatial autocorrelation terms into the GPI model.

Finally, in the case study of this manuscript, GPI model employ a decision tree model for spatial discretization. We selected this approach because it explicitly divides the space into multiple subzones in a highly interpretable manner. However, the decision tree results can be sensitive to the complexity of the tree splits, which is controlled by a hyperparameter. In case study on homelessness rates, we experimented with different complexity parameters ranging from 0.001 to 0.1 with an interval of 0.002. The PD values remained relatively stable, varying only slightly from 0.405 to 0.380. As a result, we selected a PD value within this range. However, some uncertainty remains regarding the future application of the GPI model. Additional methods, such as k-means clustering and Support Vector Machines, could also be explored to ensure more robust results.

7. Conclusion

In this study, we developed the GPI model to explore spatial relationships among various geographical variables. The model emphasizes the spatial patterns of geographical variables under the interactions of explanatory variables for exploring spatial association. By utilizing SSH and SHAP methodology, we quantified spatial associations and interactions within the GPI model. The model effectively identifies spatial associations for individual and multiple variables. Our case study demonstrates the effectiveness of the GPI model in revealing spatial associations, accommodating spatial interactions, and uncovering non-linear relationships. Overall, the GPI model offers enhanced explanatory power and adaptability, enriching our understanding of complex geographical relationships and providing valuable insights for geographical research and analysis. In future work, cautiously generalizing the GPI model's effectiveness is critical. Moreover, combining GPI with multivariate visualization methods may facilitate a deeper understanding of the spatial patterns and interactions among geographical variables.

Acknowledgments

We thank the anonymous reviewers for their constructive comments and suggestions.

Disclosure statement

No conflict of interest exists in this manuscript, and the manuscript was approved by all authors for publication.

Funding

Yang Li is supported by the China Postdoctoral Science Foundation (Grant No. 2024M764072).

Notes on contributors

Peng Luo is a Postdoctoral Research Fellow at MIT Senseable City Lab and was a visiting scholar at University of Oxford. He holds a Ph.D. from the Chair of Cartography and Visual Analytics at

the Technical University of Munich. His research centers on Spatial data science, GeoAI, and explainable and uncertainty-aware spatial modeling. Email: pengluo@mit.edu

Yang Li is a Postdoctoral Research Fellow at Beihang University and received his Ph.D. from Beijing Normal University. His research focuses on intelligent interpretation of remote sensing big data, geospatial modeling, and explainable GeoAI. Email: isliyang@buaa.edu.cn

Yongze Song is a Senior Lecturer at Curtin University. His research interests include spatial statistics, geospatial intelligence, sustainable infrastructure and sustainable development. He servers as an Associate Editor for the journals GIScience & Remote Sensing, and the International Journal of Applied Earth Observation and Geoinformation. Email: Yongze.Song@curtin.edu.au

Ziqi Li is an Assistant Professor in quantitative geography at Florida State University (FSU). His research focuses on the methodological development of spatially explicit and interpretable statistical/machine learning models to investigate human behavior across space and place. He is one of the primary developers of Multi-scale Geographically Weighted Regression (MGWR) and Python Spatial Analysis Library (PySAL). Email: Ziqi.Li@fsu.edu

Liqiu Meng is a professor of Cartography at the Technical University of Munich, and a member of German National Academy of Sciences. She is serving as Vice President of the International Cartographic Association. Her research interests include geodata integration, mobile map services, multimodal navigation algorithms, geovisual analytics, and ethical concerns in social sensing. Email: liqiu.meng@tum.de.

ORCID

Yongze Song http://orcid.org/0000-0003-3420-9622
Ziqi Li http://orcid.org/0000-0002-6345-4347
Liqiu Meng http://orcid.org/0000-0001-8787-3418

Data and codes availability statement

The data and codes that support the findings of the present study are available on Figshare at https:///doi.org/10.6084/m9.figshare.24894927.

References

Anselin, L., 1988. *Spatial econometrics: methods and models*. Vol. 4. Dordrecht: Springer Science & Business Media.

Anselin, L., 1989. *What is special about spatial data? alternative perspectives on spatial data analysis (89–4)*. UC Santa Barbara: National Center for Geographic Information and Analysis.

Anselin, L., 1995. Local indicators of spatial association—lisa. *Geographical Analysis*, 27 (2), 93–115.

Anselin, L., 2010. Thirty years of spatial econometrics. *Papers in Regional Science*, 89 (1), 3–26.

Anselin, L., and Amaral, P., 2024. Endogenous spatial regimes. *Journal of Geographical Systems*, 26 (2), 209–234.

Apté, C., and Weiss, S., 1997. Data mining with decision trees and decision rules. *Future Generation Computer Systems*, 13 (2-3), 197–210.

Arbia, G., 2006. *Spatial econometrics: statistical foundations and applications to regional convergence*. Berlin, Heidelberg: Springer Science & Business Media.

Australian Bureau of Statistics 2016. Census of population and housing: Estimating homelessness. URL https://www.abs.gov.au/statistics/people/housing/estimating-homelessness-census/2016

Brunsdon, C., Fotheringham, A.S., and Charlton, M.E., 1996. Geographically weighted regression: a method for exploring spatial nonstationarity. *Geographical Analysis*, 28 (4), 281–298.

Caton, C.L., *et al.*, 2005. Risk factors for long-term homelessness: Findings from a longitudinal study of first-time homeless single adults. *American Journal of Public Health*, 95 (10), 1753–1759.
Chen, T., and Guestrin, C., 2016, August. XGBoost: A scalable tree boosting system. *In*: *Proceedings of the 22nd ACM SIGKDD international conference on knowledge discovery and data mining*, San Francisco, California, USA. New York, NY: Association for Computing Machinery, 785–794.
Comber, A.J., *et al.*, 2021. The forgotten semantics of regression modeling in geography. *Geographical Analysis*, 53 (1), 113–134.
De Marsily, G., *et al.*, 2005. Dealing with spatial heterogeneity. *Hydrogeology Journal*, 13 (1), 161–183.
Fotheringham, A.S., Brunsdon, C., and Charlton, M., 2000. *Quantitative geography: perspectives on spatial data analysis*. London; Thousand Oaks, CA: Sage.
Fotheringham, A.S., Brunsdon, C., and Charlton, M., 2003. *Geographically weighted regression: the analysis of spatially varying relationships*. Chichester, West Sussex, England: John Wiley & Sons.
Fotheringham, A.S., and Li, Z., 2023. Measuring the unmeasurable: Models of geographical context. *Annals of the American Association of Geographers*, 113 (10), 2269–2286.
Getis, A., and Ord, J.K., 1992. The analysis of spatial association by use of distance statistics. *Geographical Analysis*, 24 (3), 189–206.
Goodchild, M.F., 2004. The validity and usefulness of laws in geographic information science and geography. *Annals of the Association of American Geographers*, 94 (2), 300–303.
Griffith, D.A., 2003. *Spatial autocorrelation and spatial filtering*. Berlin, Heidelberg: Springer.
Guo, H., Python, A., and Liu, Y., 2023. Extending regionalization algorithms to explore spatial process heterogeneity. *International Journal of Geographical Information Science*, 37 (11), 2319–2344.
Hu, X., *et al.*, 2025. A local indicator of stratified power. *International Journal of Geographical Information Science*, 39 (4), 925–943.
LeSage, J.P., and Fischer, M.M., 2008. Spatial growth regressions: model specification, estimation and interpretation. *Spatial Economic Analysis*, 3 (3), 275–304.
Li, Y., *et al.*, 2023. A locally explained heterogeneity model for examining wetland disparity. *International Journal of Digital Earth*, 16 (2), 4533–4552.
Li, Z., 2022. Extracting spatial effects from machine learning model using local interpretation method: An example of shap and xgboost. *Computers, Environment and Urban Systems*, 96, 101845.
Li, Z., 2023. Geoshapley: A game theory approach to measuring spatial effects in machine learning models.
Liu, L., 2024. An ensemble framework for explainable geospatial machine learning models. *International Journal of Applied Earth Observation and Geoinformation*, 132, 104036.
Lou, X., Luo, P., and Meng, L., 2024. Geoconformal prediction: a model-agnostic framework of measuring the uncertainty of spatial prediction. arXiv Preprint arXiv:2412.08661.
Lundberg, S.M., *et al.*, 2017. A unified approach to interpreting model predictions. *In*: *Advances in neural information processing systems* 30. Long Beach, CA: Curran Associates, Inc., 4765–4774. http://papers.nips.cc/paper/7062-a-unified-approach-to-interpreting-model-predictions.pdf
Lundberg, S.M., *et al.*, 2020. From local explanations to global understanding with explainable ai for trees. *Nature Machine Intelligence*, 2 (1), 56–67.
Luo, P., *et al.*, 2022. Identifying determinants of spatio-temporal disparities in soil moisture of the northern hemisphere using a geographically optimal zones-based heterogeneity model. *ISPRS Journal of Photogrammetry and Remote Sensing*, 185, 111–128.
Luo, P., *et al.*, 2023. A generalized heterogeneity model for spatial interpolation. *International Journal of Geographical Information Science*, 37 (3), 634–659.
Luo, H., Luo, P., and Meng, L., 2025. A robust geographically optimal zones-based heterogeneity model for analyzing the spatial determinants of national traffic accidents. *GIScience & Remote Sensing*, 62 (1), 2448283.
Luo, P., and Song, Y., 2021. A spatial second-order non-stationary interpolation method for large area mapping. *Abstracts of the ICA*, 3, 1–1.
Luo, P., Song, Y., and Wu, P., 2021. Spatial disparities in trade-offs: economic and environmental impacts of road infrastructure on continental level. *GIScience & Remote Sensing*, 58 (5), 756–775.

Oshan, T.M., *et al.*, 2019. mgwr: A python implementation of multiscale geographically weighted regression for investigating process spatial heterogeneity and scale. *ISPRS International Journal of Geo-Information*, 8 (6), 269.

Parkinson, S., *et al.*, 2019. *The changing geography of homelessness: a spatial analysis from 2001 to 2016*. Australian Housing and Urban Research Institute Limited, Melbourne.

Sachdeva, M., *et al.*, 2022. Are we modelling spatially varying processes or non-linear relationships? *Geographical Analysis*, 54 (4), 715–738.

Shapley, L.S., *et al.*, 1953. A value for n-person games.

Song, Y., 2023. Geographically optimal similarity. *Mathematical Geosciences*, 55 (3), 295–320.

Song, Y., *et al.*, 2020. An optimal parameters-based geographical detector model enhances geographic characteristics of explanatory variables for spatial heterogeneity analysis: Cases with different types of spatial data. *GIScience & Remote Sensing*, 57 (5), 593–610.

Štrumbelj, E., and Kononenko, I., 2014. Explaining prediction models and individual predictions with feature contributions. *Knowledge and Information Systems*, 41 (3), 647–665.

Wang, J., *et al.*, 2010. Geographical detectors-based health risk assessment and its application in the neural tube defects study of the Heshun region, China. *International Journal of Geographical Information Science*, 24 (1), 107–127.

Wang, J., *et al.*, 2022. Statistics for spatially stratified heterogeneous data. arXiv Preprint arXiv: 2211.16918.

Wang, J., and Xu, C., 2017. Geodetector: Principle and prospective. *Acta Geogr. Sin*, 72 (01), 116–134.

Yang, L., *et al.*, 2024. A spatio-temporal unmixing with heterogeneity model for the identification of remotely sensed modis aerosols: Exemplified by the case of Africa. *International Journal of Applied Earth Observation and Geoinformation*, 132, 104068.

Zhang, Z., *et al.*, 2023. Geocomplexity explains spatial errors. *International Journal of Geographical Information Science*, 37 (7), 1449–1469.

Zhang, Z., Li, Z., and Song, Y., 2024. On ignoring the heterogeneity in spatial autocorrelation: consequences and solutions. *International Journal of Geographical Information Science*, 38 (12), 2545–2571.

Zhu, D., *et al.*, 2022. Spatial regression graph convolutional neural networks: A deep learning paradigm for spatial multivariate distributions. *GeoInformatica*, 26 (4), 645–676.

Zhu, T., Fonseca De Lima, C.F., and De Smet, I., 2021. The heat is on: how crop growth, development, and yield respond to high temperature. *Journal of Experimental Botany*, 72 (21), 7359–7373.

Appendix

Table A1. Key abbreviations.

Abbreviation	Full name
GPI	Geographical Pattern Interaction
GOZH	Geographically Optimal Zones-based Heterogeneity Model (Luo *et al.* 2022a)
GWR	Geographically Weighted Regression (Fotheringham *et al.* 2003)
MGWR	Multi-scale Geographically Weighted Regression (Oshan *et al.* 2019)
PD	Power of Determinant (Wang *et al.* 2010)
XGBoost	Extreme Gradient Boosting (Chen and Guestrin 2016)
SHAP	SHapley Additive exPlanations (Lundberg *et al.* 2017)